Supplementary information: Mechanisms of passivation and chloride-induced corrosion of mild steel in sulfide-containing alkaline solutions

Shishir Mundra[1,2,3], John L. Provis[1*]

[1] Department of Materials Science and Engineering, The University of Sheffield, Sir Robert Hadfield Building, Sheffield, S1 3JD, United Kingdom

[2] Division 7.4, Technology of Construction Materials, Bundesanstalt für Materialforschung und -prüfung (BAM), Unter den Eichen 87, Berlin 12205, Germany

[3] Institute for Building Materials (IfB), ETH Zurich, Stefano-Franscini-Platz 3, 8093, Zurich, Switzerland

[*]Corresponding author: j.provis@sheffield.ac.uk

ORCID identifiers: 0000-0001-6559-8814 (S. Mundra); 0000-0003-3372-8922 (J. Provis)

1 Experimental Programme

Figure S1 shows the setup used for electrochemical measurements in this study. A 400 mL corrosion cell using a PGSTAT 204 potentiostat/galvanostat (Metrohm Autolab B.V.) was used in this study. Measurements were conducted using a conventional three electrode setup (electrolyte volume 250 mL), comprising a stainless-steel counter electrode, an Ag/AgCl (saturated 3 M KCl) reference electrode, and the mild steel surface (surface area: 0.287 cm^2) acting as the working electrode. The steel surface tested was the cut surface, not a curved rebar surface. The reference electrode was positioned near the surface of the working electrode by means of a Luggin capillary. All measurements were conducted at room temperature (22 ± 2 °C).

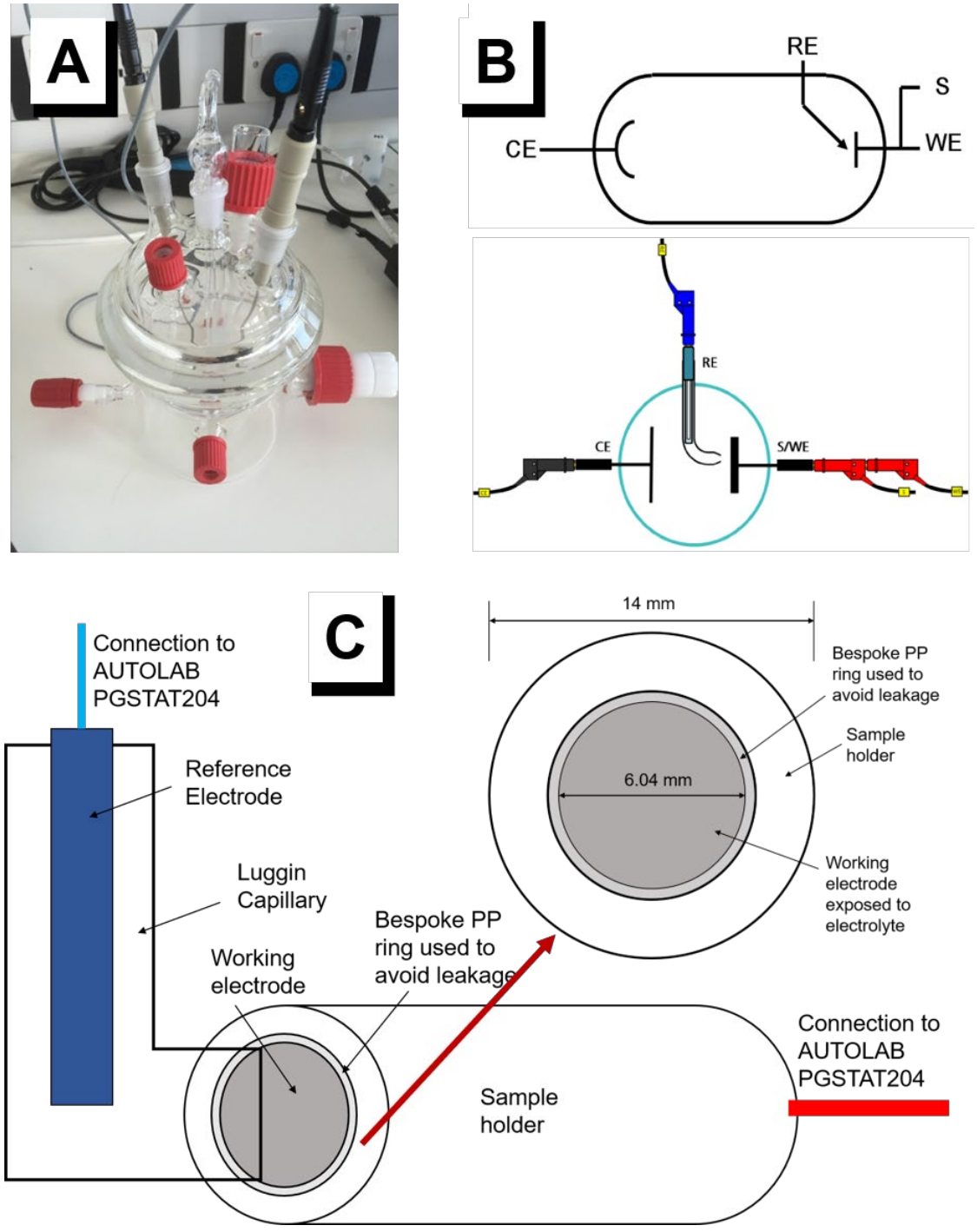

Figure S1: (A) 400 mL corrosion cell (Metrohm Autolab B.V.), (B) schematic of the three-electrode cell, where RE = reference electrode, CE = counter electrode, WE = working electrode, S = sample. (C) Schematic of the cell setup used for electrochemical testing. The Luggin capillary was positioned in front of the working electrode at a distance of 1-1.5 mm.

2 pH measurements

Table S1 shows the evolution of the pH values of alkaline solutions (0.80 M OH^-) with varying concentrations of HS^- (0 M, 0.001 M, 0.01 M, 0.09 M, 0.45 M) over a period of 28 days. The pH values correspond to the solutions to which mild steel was exposed prior to electrochemical testing.

Table S1: The evolution of pH of alkaline solutions (0.80 M OH^-) with varying concentrations of HS^- (0 M, 0.001 M, 0.01 M, 0.09 M, 0.45 M) over a period of 28 days. The pH values reported correspond to the solutions to which mild steel was exposed to prior to electrochemical tests. Values in parentheses are the standard deviations.

Time (d)	**0.80 M OH^- + 0 M HS^-**	**0.80 M OH^- + 0.001 M HS^-**	**0.80 M OH^- + 0.01 M HS^-**	**0.80 M OH^- + 0.09 M HS^-**	**0.80 M OH^- + 0.45 M HS^-**
0	13.95 (0.02)	13.96 (0.00)	13.90 (0.03)	13.90 (0.06)	13.85 (0.01)
5	13.96 (0.03)	13.96 (0.04)	13.91 (0.01)	13.90 (0.00)	13.84 (0.03)
12	13.99 (0.06)	13.95 (0.03)	13.92 (0.02)	13.90 (0.03)	13.87 (0.01)
28	13.94 (0.05)	13.95 (0.07)	13.91 (0.00)	13.90 (0.02)	13.86 (0.02)

3 Cyclic voltammetry

Figure S2 shows the first 5 scans of cyclic voltammetry conducted on mild steel exposed to (A) 1.12 M OH^- + 0.01 M HS^-, and (B) 1.36 M OH^- + 0.45 M HS^-. On comparison with Figure 2B, the current densities associated with anodic peaks I, II, III and III' were observed to increase with an increase in the [OH^-] in the electrolyte. The higher current densities (observed in Figure S2) associated with peak I are primarily due to increased competitive adsorption between OH^- and HS^- on the steel surface. As mentioned in Section 3.1.1 of the main paper, Peaks II, III and III' are related to the formation of iron oxides and hydroxides, and the current densities associated with the peaks were observed to increase with an increase in the [OH^-] in the electrolyte (as shown in Figure S2A,B and Figure 1B). This is line with [1], where an increased alkalinity in the electrolyte leads to a higher degree of passivation on the steel surface.

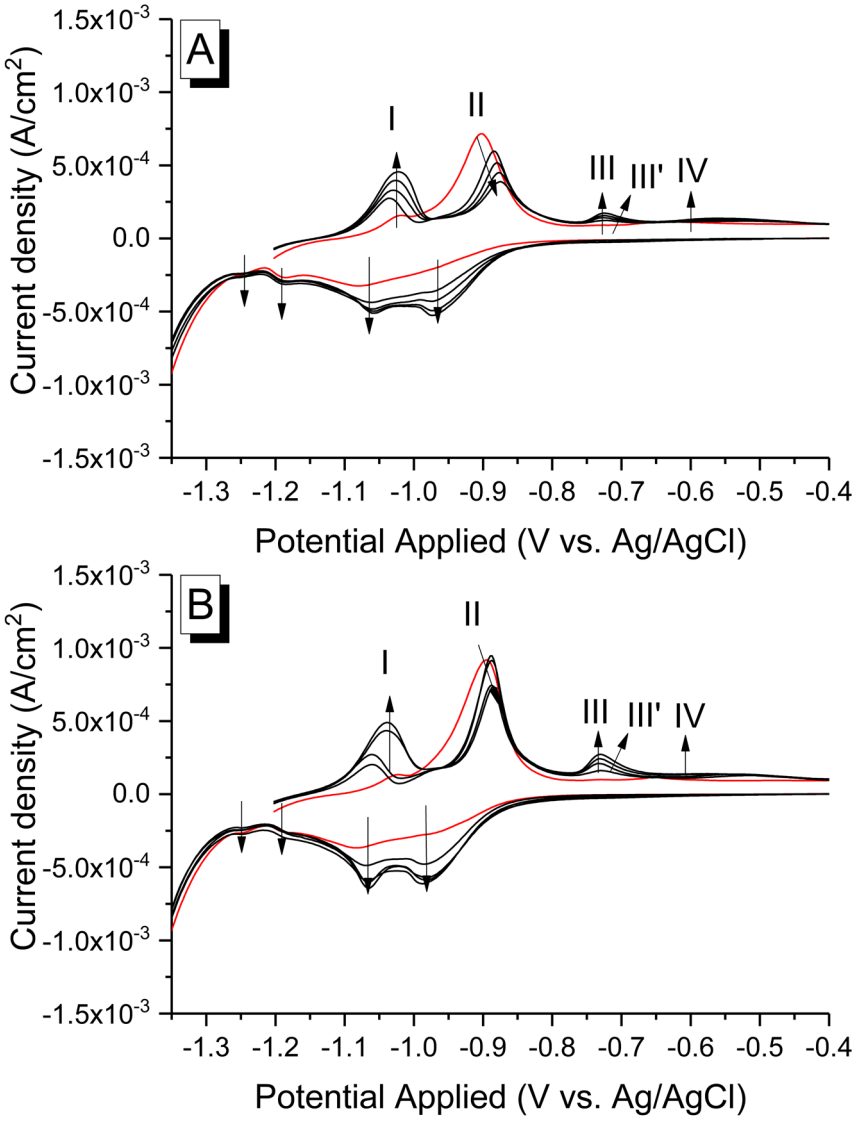

Figure S2: Cyclic voltammograms obtained for mild steel exposed to (A) 1.12 M OH^- + 0.01 M HS^-, and (B) 1.36 M OH^- + 0.45 M HS^-. Data were collected at a sweep rate of 2.5 mV/s. Arrows indicate the current response from scan numbers 1 to 5. Data from -1.50 V to -1.20 V in the anodic sweeps are omitted, to enable visibility of all peaks. The red line indicates the first scan, and subsequent scans are represented by black lines.

Figure S3 corresponds to the pH of the bulk solution in the corrosion cell measured during the first anodic scan (from -1.20 V to 0.65 V vs. Ag/AgCl) of the cyclic voltammetry test for mild steel in alkaline solution (0.80 M OH^-) with varying concentrations of sulfide (0 M, 0.01 M and 0.45 M HS^-). These measurements correspond to the results of the cyclic voltammetry

tests shown in Figure 1 (main paper). The pH measurements obtained using a digital pH meter (Oakton Acorn Series), calibrated with reference standard pH buffer solutions of pH 4, 7 and 10. It is to be noted that the accuracy of glass electrodes used to measure the pH of highly alkaline solutions, as is the case in this study, is questionable and is commonly referred to as the "alkaline error" [2]. Additionally, due to instrumental constraints the recorded pH values are representative of the bulk solution instead of the pH immediately at the steel/solution interface.

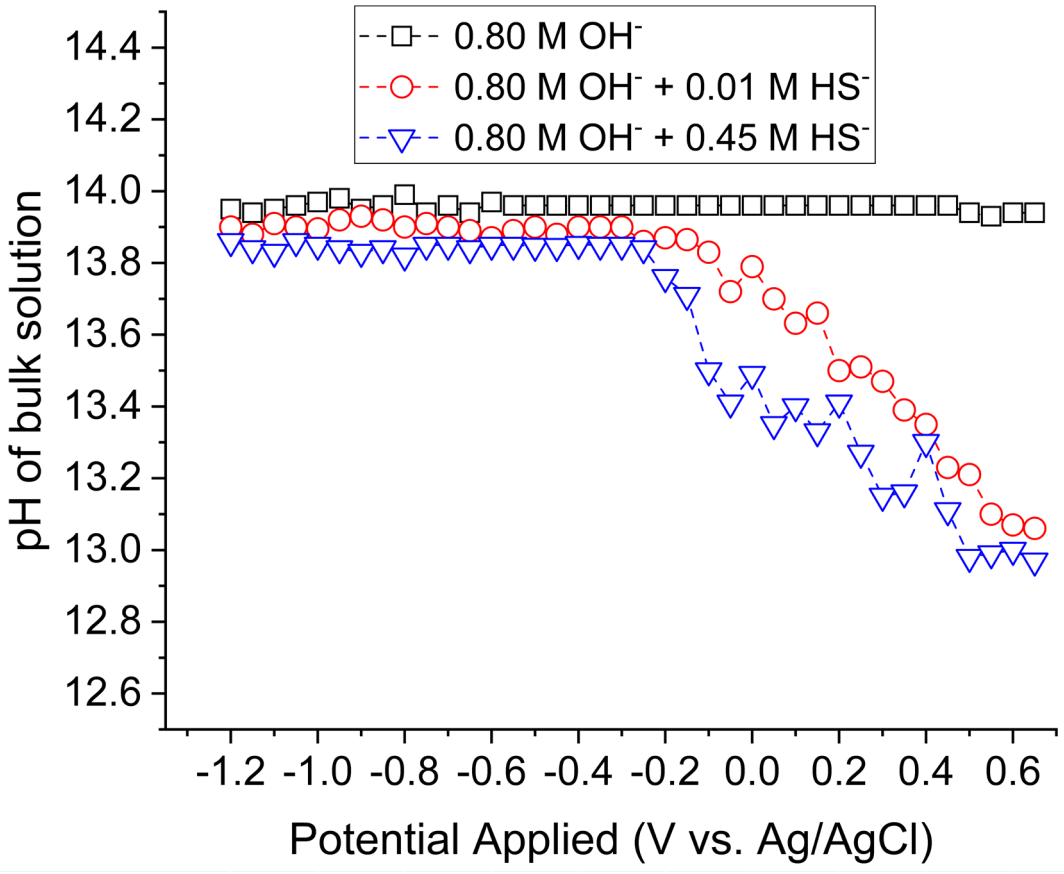

Figure S3: Measured pH of the bulk solution in the corrosion cell during the first anodic scan of the cyclic voltammetry test for mild steel exposed to 0.80 M OH^-, 0.80 M OH^- + 0.01 M HS^-, and 0.80 M OH^- + 0.45 M HS^-.

4 X-ray photoelectron spectroscopy

Figure S4 and Figure S5 show the S 2*p* and Fe 2$p_{3/2}$ XPS spectra of steel specimens exposed to alkaline sulfide solutions for 12 and 28 days, respectively. Measurements and analysis of data were conducted as described in Section 2.2.3.

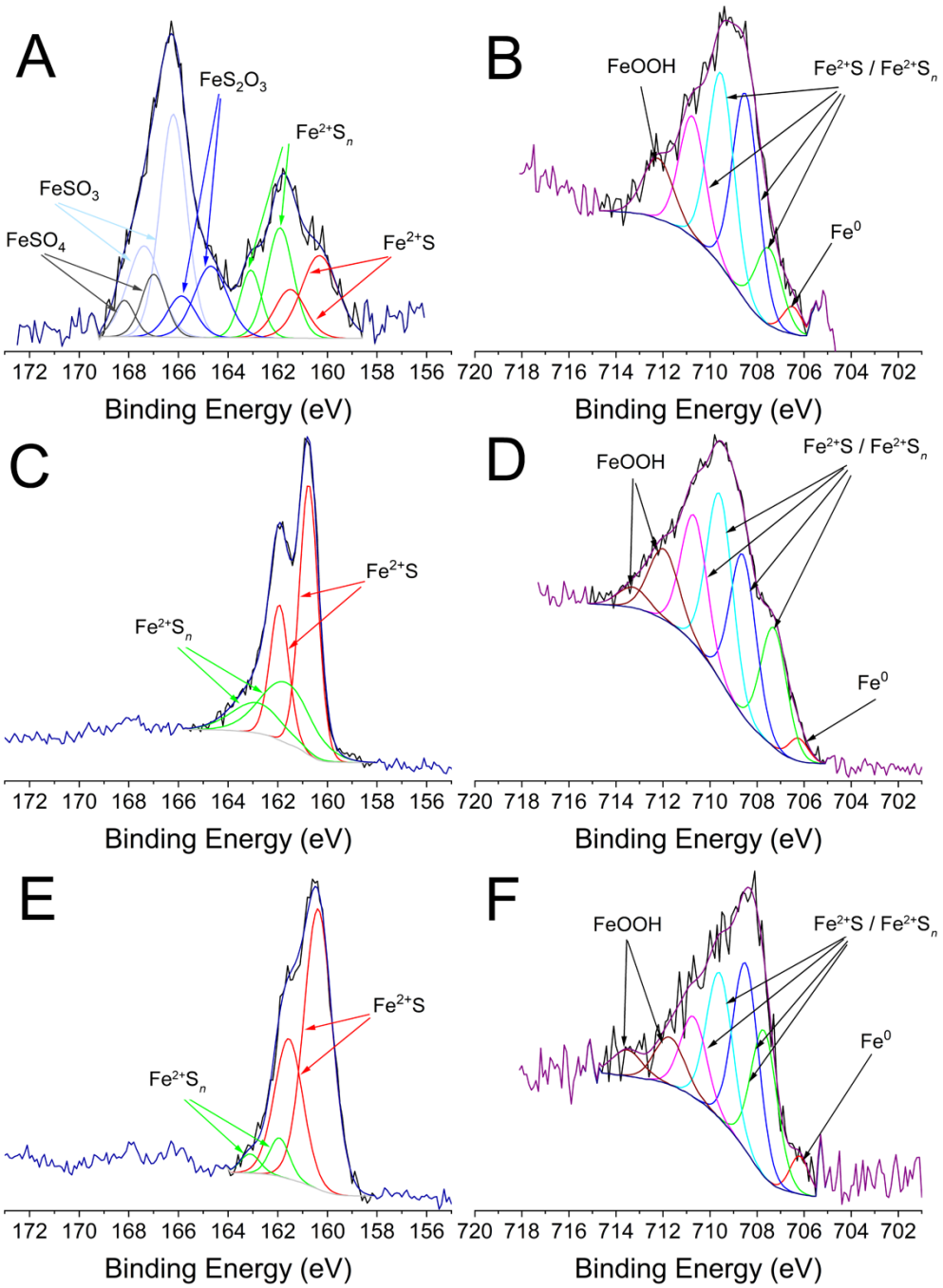

Figure S4: S 2*p* and Fe 2$p_{3/2}$ XPS spectra of steel specimens exposed to alkaline sulfide solutions for 12 days. (A) and (B) show the S 2*p* and Fe 2$p_{3/2}$ spectra, respectively, for steel immersed in 0.80 M OH^- + 0.01 M HS^-; (C) and (D) show the S 2*p* and Fe 2$p_{3/2}$ spectra, respectively, for steel immersed in 0.80 M OH^- + 0.09 M HS^-; and (E) and (F) show the S 2*p* and Fe 2$p_{3/2}$ spectra, respectively, for steel immersed in 0.80 M OH^- + 0.45 M HS^-.

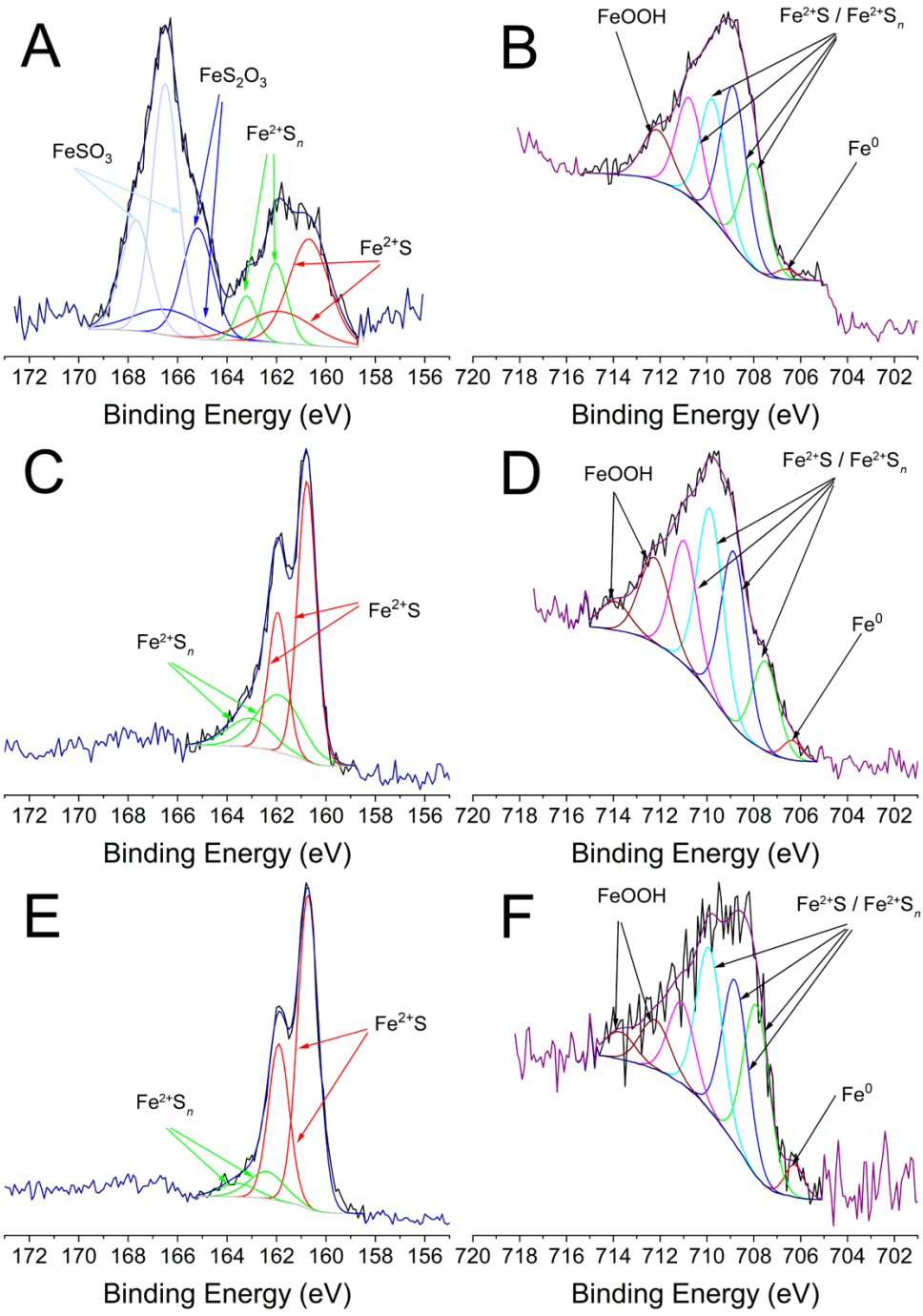

Figure S5: S 2*p* and Fe 2*p*$_{3/2}$ XPS spectra of steel specimens exposed to alkaline sulfide solutions for 28 days. (A) and (B) show the S 2*p* and Fe 2*p*$_{3/2}$ spectra, respectively, for steel immersed in 0.80 M OH^- + 0.01 M HS^-; (C) and (D) show the S 2*p* and Fe 2*p*$_{3/2}$ spectra, respectively, for steel immersed in 0.80 M OH^- + 0.09 M HS^-; and (E) and (F) show the S 2*p* and Fe 2*p*$_{3/2}$ spectra, respectively, for steel immersed in 0.80 M OH^- + 0.45 M HS^-.

5 Polarisation of inert iridium working electrode

The OCP (as shown in Figure 3 in the main paper) recorded for an inert iridium working electrode decreased upon an increase in the concentration of reduced sulfur species (0.80 M OH^-: -0.13 V vs. Ag/AgCl, 0.80 M OH^- + 0.01 M HS^-: -0.47 V vs. Ag/AgCl, and 0.80 M OH^- + 0.45 M HS^-: -0.70 V vs. Ag/AgCl), indicative of a reduction in the concentration of dissolved oxygen in the aqueous electrolyte. In the event of a reduction in the concentration of dissolved oxygen in the electrolyte, one would typically expect a concurrent reduction in the potential and the corrosion rate or corrosion current density. However, the current density of the steel reinforcement was observed to increase upon an increase in the concentration of reduced sulfur species (as shown in Figure 4 in the main paper), contrary to the theory. A progressive increase in the current densities (and no passivation) with an increase in the sulfide concentrations (reduction in the dissolved oxygen concentration) in the electrolyte, as seen in the anodic polarisation curves for steel immersed in alkaline solutions with and without sulfide (Figure 4 – main paper), could presumably be explained by:

1. An increase in the [HS^-] in alkaline solution leads to increased anodic dissolution of Fe, resulting in the uniform corrosion of the steel surface under study, or,

2. The application of an external voltage in the anodic polarisation test results in the oxidation of HS^- in the aqueous electrolyte, thereby causing an increase in the current density. Therefore, the redox couple $S^{2-} \rightarrow S^x$ (x > 2-) at the electrolyte-electrode interface acts as an additional anode, contributing to the anodic current response of the system under study.

To understand whether each of the above-mentioned points could be responsible for the observation of increased current densities in alkaline sulfide rich solutions, anodic polarisation tests on an inert Iridium working electrode (exposed to solutions with and without sulfide) were performed. Figure S6 shows the anodic polarisation curves obtained for an inert Iridium working electrode exposed to alkaline solutions (0.80 M OH^-) with varying concentrations of sulfide (0 M, 0.01 M and 0.45 M HS^-). The electrolytes were prepared using reagent grade NaOH (Sigma Aldrich) and $Na_2S \cdot 9H_2O$ (Alfa Aesar). Measurements were conducted in a 500 ml corrosion cell, using a Gamry Reference 600 potentiostat. Measurements were conducted using a conventional three electrode setup (electrolyte volume 500 mL), comprising a Pt-mesh

counter electrode, an Ag/AgCl (saturated 3 M KCl) reference electrode, and an inert Iridium mesh (surface area: 103 cm^2) acting as the working electrode. All measurements were conducted under room temperature (22 ± 2 °C). Upon exposure to each of the solutions, the OCP of the inert iridium electrode was monitored for 30 mins. The specimens were anodically polarised by increasing the potential from the -10 mV vs. OCP to +1.0 V vs. OCP, with the step potential and scan rate set at 0.244 mV and 0.167 mV/s.

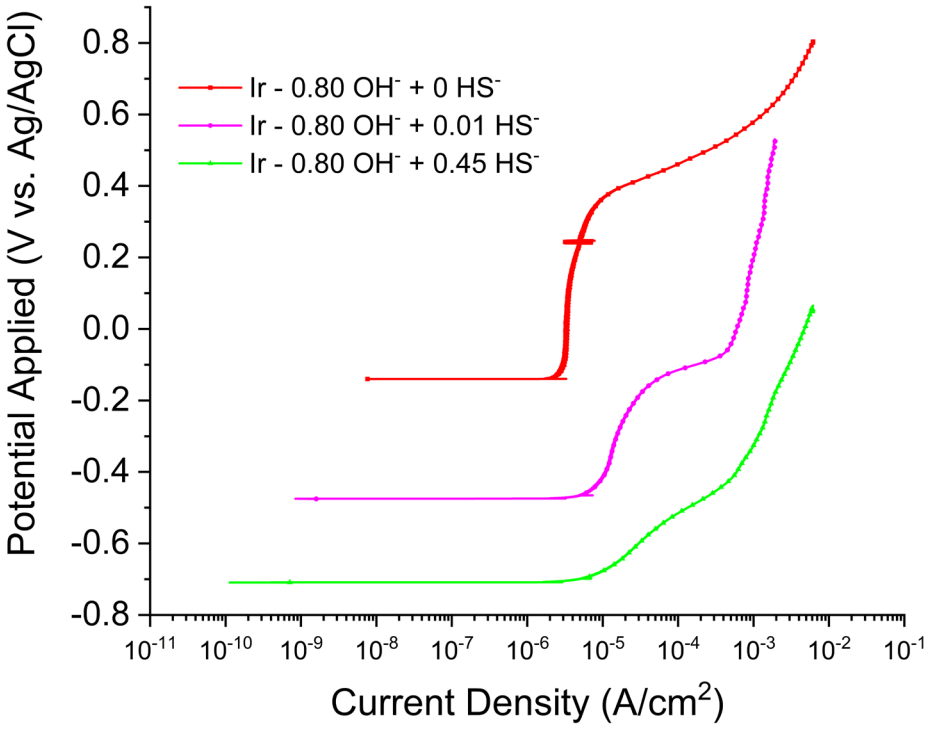

Figure S6: Anodic polarisation curves of an inert Iridium working electrode (surface area: 103 cm^2) when exposed to solutions with compositions 0.80 M NaOH, 0.80 M NaOH + 0.01 M $Na_2S{\cdot}9H_2O$, and 0.80 M NaOH + 0.45 M $Na_2S{\cdot}9H_2O$.

Anodic polarisation curves shown in Figure S6 for an inert Iridium electrode clearly indicate an increase in the anodic current density with an increase in the concentration of HS^-, very similar to the observations made for steel in sulfide containing alkaline solutions. In the absence of dissolution of the inert iridium electrode, the higher anodic current density observed in the polarisation curves for iridium in sulfide containing solutions than sulfide free solution, clearly suggests that the current response being dominated by the oxidation of something other than

the working electrode and most likely the reduced sulfur species at the electrolyte-electrode interface. The observation from Figure S6 can be used to explain the increased current density seen during the anodic polarisation of steel (Figure 4 – main paper) in highly alkaline sulfide containing solutions.

For the progressive increase in the current density with an increase in the [HS^-] in alkaline solution to be related to increased anodic dissolution of Fe (as noted in point 1 - mentioned above), one would expect the current density to be fairly similar irrespective of the solution used when anodic polarisation is performed on an inert electrode. The results in Figure S6 however, negate this presumption and it can be confidently claimed that higher current densities observed in the anodic polarisation curves upon increasing the sulfide concentration do not relate to the dissolution of Fe or the "uniform corrosion" of the steel. Instead, the results from Figure S6 indicate that the upon application of an external anodic potential, the higher current densities are related to the oxidation of aqueous reduced sulfur species at the electrolyte-electrode interface, as presumed in the above mentioned point 2.

6 Polarisation resistance and corrosion current density

It is a well-known fact that the applicability of R_p and i_{corr} values obtained from LPR in quantitatively assessing chloride-induced or macro-cell corrosion is limited, and only provide qualitative indicatory information. However, given the partially non-destructive nature of the LPR test and its relative ease in its application, its use in studies concerning chloride-induced corrosion of steel-reinforcements embedded in mortars/concretes continues to be widespread. To this end, it was considered noteworthy to conduct LPR tests (experimental parameters described in Section 2.2.2) on steel exposed to alkaline solutions with and without sulfide and highlight the complexities in the interpretation of the results obtained in electrolytes containing significant quantities of sulfide. Corrosion current densities (i_{corr}) were calculated using Eq. 2 (main paper) from the measured R_p values, using proportionality constants B proposed in the literature [3,4], of 26 and 52 mV for mild steel being in the active and passive states, respectively, as is commonly done for tests conducted in steel reinforced concretes or in simulated pore solutions of concretes.

Figure S7 shows the measured R_p values obtained via the linear polarisation resistance method and the corresponding calculated corrosion current densities (i_{corr}) in μA/cm^2. Figure S7A highlights that no apparent correlation between R_p and HS^-, OH^-, and Cl^- in the electrolyte, and of the time of exposure was observed, other than the fact that the samples undergoing pitting corrosion had low R_p values, as expected. However, the R_p values did not exhibit a notable drop at any particular threshold chloride concentration. Like R_p, the calculated i_{corr} values also do not exhibit a simple relationship between i_{corr} and HS^-, OH^-, and Cl^- in the electrolyte. It is important to note that the values of B used in this study to calculate i_{corr}, in the modified Stern-Geary equation (Eq. 2 – main paper), are those which are conventionally employed in mild steel embedded in PC-based concretes or exposed to their representative pore solutions. In the case of steel-reinforced alkali-activated fly ashes (low-Ca alkali-activated materials) [5], the values of the cathodic and anodic Tafel constants have been found to deviate substantially from those reported in [3,4]. The validity of these Tafel constants (or B for PC-based concretes) in the case of steel exposed to simulated pore solutions of AAS – where in addition to the redox couple Fe/Fe^{2+}, sulfide species in the pore solutions can also oxidise – is unknown. Therefore, it is important to not compare the R_p or i_{corr} of active/passive steel in PC based concretes (or simulated pore solutions) directly to those of active/passive steel in AAS concretes (or simulated pore solutions), especially when an additional redox active species is present in the electrolyte. In addition, Figure S7 highlights the fact that the measured values of R_p using LPR and calculated i_{corr} for steel in solutions containing various HS^- and Cl^- does not indicate whether steel is in the active/passive state.

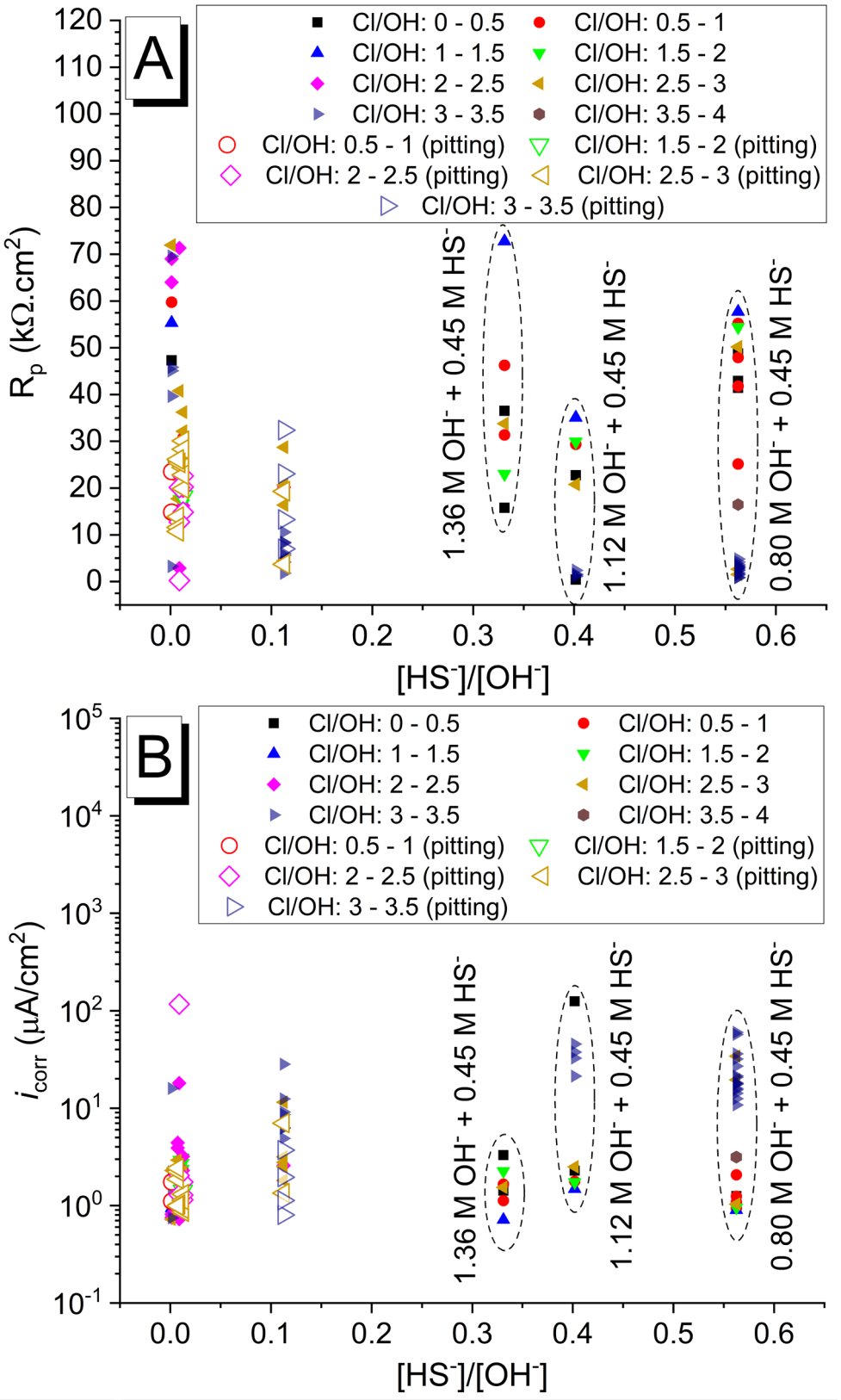

Figure S7: Measured R_p values obtained through linear polarisation resistance method, and corresponding calculated i_{corr} (μA/cm^2). The i_{corr} values were calculated using the modified

Stern-Geary equation with proportionality constants *B* taken as 26 and 52 mV for active and passive states of the steel reinforcement, respectively. The solid symbols denote the steel samples exhibiting no corrosion, whereas the hollow symbols indicate stable or metastable chloride-induced pitting.

7 References

[1] S. Mundra, M. Criado, S.A. Bernal, J.L. Provis, Chloride-induced corrosion of steel rebars in simulated pore solutions of alkali-activated concretes, Cem. Concr. Res. 100 (2017) 385–397.

[2] D.J. Graham, B. Jaselskis, C.E. Moore, Development of the glass electrode and the pH response, J. Chem. Educ. 90 (2013) 345–351.

[3] C. Andrade, C. Alonso, Corrosion rate monitoring in the laboratory and on-site, Constr. Build. Mater. 10 (1996) 315–328.

[4] C. Andrade, J.A. González, Quantitative measurements of corrosion rate of reinforcing steels embedded in concrete using polarization resistance measurements, Mater. Corros. 29 (1978) 515–519.

[5] M. Babaee, A. Castel, Chloride-induced corrosion of reinforcement in low-calcium fly ash-based geopolymer concrete, Cem. Concr. Res. 88 (2016) 96–107.